An immune escape-related gene signature for predicting the prognostic and immune microenvironment in osteosarcoma

Chen Meng[1], Chuan Li[2,3], Yongqing Xu[2]*

[1]Department of Orthopedic, Affiliated Hospital of Yangzhou University, Yangzhou China
[2]920th Hospital of Joint Logistics Support Force of Chinese People's Liberation Army, Xishan District, Kunming, Yunnan, China
[3]Kunming Institute of Zoology, Chinese Academy of Sciences, Kunming, Yunnan, China

Submitted: 22 May 2024; **Accepted:** 5 January 2025
Online publication:

Arch Med Sci
DOI: https://doi.org/10.5114/aoms/199786

***Corresponding author:**
Yongqing Xu
920th Hospital of Joint Logistics Support Force of Chinese People's Liberation Army,
212 Daguan Road
Xishan District, Kunming
Yunnan, China
E-mail: xyongqingkm@163.com

Abstract

Introduction: This study aimed to develop an immune escape-related gene signature for prognostic prediction and clarification of the immune microenvironment in osteosarcoma, a predominant malignant bone tumor in pediatric and adolescent populations.
Material and methods: This study used transcriptomic and genomic data from various databases (Therapeutically Applicable Research to Generate Effective Treatments and Gene Expression Omnibus). A prognostic model was established using the least absolute shrinkage and selection operator method, followed by rigorous statistical analysis. Additionally, the study involved the investigation of differential pathways and single-cell data analysis to understand the immune escape mechanisms in osteosarcoma.
Results: The study successfully developed an immune escape-related gene model that stratifies patients with osteosarcoma into different prognostic groups with significant survival differences. It indicated that higher immune escape-related gene scores were associated with poor survival outcomes. Additionally, the model demonstrated efficacy in predicting the complexity and variability of the immune microenvironment in osteosarcoma, correlating with different immune cell infiltrations and immunotherapy responses. Furthermore, single-cell analysis revealed distinct molecular signatures and pathways associated with immune escape, emphasizing potential therapeutic targets in osteosarcoma management.
Conclusions: The immune escape-related gene model provides a novel approach to understanding and predicting osteosarcoma prognosis. This model serves as a valuable tool for determining potential therapeutic targets and developing personalized treatment strategies. It emphasizes the importance of immune escape mechanisms in osteosarcoma progression and treatment.

Key words: osteosarcoma, immune escape, immune microenvironment, single-cell analysis.

Introduction

Not only is osteosarcoma the most prevalent primary malignant bone tumor in children and adolescents, but its highly aggressive nature and rapid growth also contribute to a poor prognosis and a high rate of metastasis [1]. Studies have revealed that the lungs are the most predomi-

nant metastasis site in osteosarcoma, which further complicates treatment and reduces survival rates [2, 3]. The overall survival rate for osteosarcoma has shown limited improvement in recent years, especially in patients with advanced or recurrent disease, despite the use of neoadjuvant chemotherapy and extensive surgical resection [4, 5]. Therefore, establishing new methods for early diagnosis and prognostic indicators is crucial for improving the survival rates of patients with osteosarcoma. Research indicates that tumor cells evade the immune system's surveillance through mechanisms such as altering antigen presentation, producing immunosuppressive factors, or modifying the tumor microenvironment, in terms of tumor immune evasion [6, 7]. Initially, the mutation and evasion mechanisms of the tumor cells themselves were widely believed to be the main factors in tumor immune evasion. However, with further research, increasing evidence indicates that the tumor microenvironment, including immune cells, stromal cells, and cytokines, plays a vital role in this process [8]. Therefore, the present study uses cutting-edge transcriptomic and single-cell genomic technologies to develop a gene model pertinent to immune evasion [9]. This research not only investigates the role of immune evasion-related genes in osteosarcoma prognosis but also assesses their predictive value within the immune microenvironment by analyzing samples of patients with osteosarcoma, thereby providing novel insights and strategies for osteosarcoma treatment [10].

This investigation helps in deepening the understanding of tumor immune evasion's role in osteosarcoma progression, thereby providing a theoretical foundation for developing new therapeutic approaches. As this tumor demonstrates significant genetic heterogeneity, which limits the efficacy of standardized treatment approaches and potentially causes substantial variability in individual treatment responses, we explore more deeply the background and challenges of osteosarcoma [9]. Moreover, the success rates of standard treatments are further diminished for recurrent or refractory osteosarcoma, emphasizing the need for more personalized and targeted therapeutic strategies [11]. This is partly caused by the complex and variable immune microenvironment of osteosarcoma, characterized by immune cell type and cytokine diversity, whose interactions and effects on tumor growth remain unclear [12]. This study aims to determine the complexity and dynamic changes of the immune microenvironment in osteosarcoma by developing a gene model associated with immune evasion, considering the aforementioned challenges. This study aims to identify and characterize those immune evasion-related genes that play a pivotal role in osteosarcoma through the integrated application of transcriptomics and single-cell genomics. This approach not only facilitates an understanding of key regulatory factors in the osteosarcoma immune microenvironment but also reveals new biomarkers and therapeutic targets, thereby supporting the development of more effective personalized treatment strategies [13].

In summary, this study provides a novel perspective by examining the role of immune evasion mechanisms in osteosarcoma, potentially providing new strategies and directions for treating this complex and challenging malignancy.

Material and methods

Dataset download and processing

We collected clinical information and RNA sequencing data for patients with osteosarcoma from the Therapeutically Applicable Research to Generate Effective Treatments (TARGET, [https://ocg.cancer.gov/programs/target]) database. Following meticulous curation, the final training dataset comprised exclusively 84 osteosarcoma samples with comprehensive records of age, gender, and metastatic status. Moreover, we sourced additional datasets from the Gene Expression Omnibus (GEO, [https://www.ncbi.nlm.nih.gov/geo/]) database, specifically GSE16091 and GSE162454. The GSE16091 dataset comprises 34 osteosarcoma samples, processed with the Affymetrix Human Genome U133A Array sequencing platform. We downloaded scRNA-seq data for three osteosarcoma samples (GSM4952363, GSM4952364, and GSM4952365) from GSE162454 for single-cell analysis. In this process, we determined 182 genes associated with immune escape, which are detailed in Supplementary Table SI.

Construction and validation of a prognostic model

Initially, a prognostic model was developed using the TARGET dataset as the training set. We utilized the "glmnet" package in R to apply the least absolute shrinkage and selection operator (LASSO) method for refining the preliminary selection of prognostic immune escape-related genes. The developed prognostic model was succinctly represented by the following formula: $riskScore = \Sigma_j^n (COEF_i \times X_i)$, where X signifies the expression level of each gene and Coef denotes the respective regression coefficient assigned to each gene after applying LASSO regression. We used this prognostic model to calculate the risk score for each patient with osteosarcoma. Patients were then categorized into high- and low-risk groups based on their median scores. Addi-

tionally, the sample collection from GSE16091 was used as an external validation cohort, enabling us to confirm the predictive precision of our model.

Prognostic value of the immune escape-related gene model

We illustrated the survival durations of the two patient groups with Kaplan-Meier curves. We applied the log-rank test to evaluate the disparities in survival times between these groups. Additionally, the efficacy of the prognostic model in predicting outcomes was assessed with time-dependent receiver operating characteristic (ROC) analysis.

Differential gene analysis

Differential gene expression was analyzed using the limma package in R [14], focusing on genes that demonstrate a logarithmic fold change (Log_2FC) absolute value of > 0.5 and a *p*-value of < 0.05.

Comparison of immune infiltration levels among immune escape-related gene groups

The tumor immune microenvironment (TIME) is crucial in affecting tumor progression and the effectiveness of chemotherapy. We initially computed stromal, immune, and Estimation of Stromal and Immune cells in Malignant Tumor tissues using Expression data (ESTIMATE) scores with the ESTIMATE algorithm [15] to analyze immune infiltration differences among subtypes. We then used the ssGSEA method to ascertain the enrichment scores for 28 immune cell types based on the gene expression profiles in osteosarcoma samples. Furthermore, we established 29 immune-related gene sets to facilitate the analysis of immune cells and their functions in the high- and low-risk groups.

Functional enrichment analysis of the immune escape-related gene model

We pinpointed genes with differential expression (DEGs) between the high- and low-risk groups related to immune escape. These were then visualized using the "pheatmap" package in R. We sourced the gene sets "c2.cp.kegg.v7.4.symbols" and "c5.go.bp.v7.4.symbols" from the MSigDB database (https://www.gsea-msigdb.org/gsea/msigdb) for gene set variation analysis (GSVA). Furthermore, we conducted Gene Ontology (GO) and Kyoto Encyclopedia of Genes and Genomes (KEGG) enrichment analyses, employing the "clusterProfiler" and "org.Hs.eg.db" packages in R.

Single-cell data analysis

Single-cell data were processed with the Seurat package in R [16] to obtain single-cell gene expression profiles. Low-quality cells (minimum expressed genes of ≥ 10 and gene count of ≥ 200) were excluded, with the remaining cells used for bioinformatics analysis. The "NormalizedData" function was used for normalizing scRNA-seq data, and the FindVariableFeatures function determined the 5,000 most variable genes. Principal component analysis (PCA) was conducted with the "RunPCA" function. Unsupervised clustering of major cell subtypes was conducted with Seurat's FindClusters function and visualized using Uniform Manifold Approximation and Projection. Cell annotation was based on the Cellmarker database, and differential genes in high- and low-immune escape-scoring groups were determined with Seurat's FindMarkers function. GO and KEGG enrichment analyses were conducted using the "clusterProfiler" and "org.Hs.eg.db" R packages. The iTALK R package [17] was used for investigating cell communication maps.

Immunofluorescence assay

The human osteosarcoma cell line U-2 OS and osteoblast cells were employed to validate the expression levels of proteins encoded by immune escape-related genes autophagy related 7 (ATG7), suppressor of cytokine signaling 1 (SOCS1), and TNF receptor superfamily member 1A (TNFRSF1A). Cells were cultured on coverslips at 37°C with 5% CO_2, and the culture process was terminated when the cell density approached approximately 90%. Following cultivation, the cells were washed with phosphate-buffered saline (PBS) and fixed with 4% paraformaldehyde for 20 min. Subsequently, a 0.5% solution of Triton X-100 was applied to the cells for cell permeabilization for a duration of 20 min, followed by three washes with PBS. The cells were blocked with 5% bovine serum albumin (BSA) for 2 h and were incubated with primary antibodies at 4°C overnight. On the following day, the primary antibodies were removed and the cells were subjected to three washes with PBS. Fluorescently labeled secondary antibody was provided and incubated with the cells at 37°C for 1 h in the dark. Following the incubation, the cells were washed three times, and the nuclei were stained with DAPI for 5 min. Subsequently, the slides containing the cells were sealed using a solution that included anti-fluorescence quenching agents and observed utilizing a fluorescence microscope.

Statistical analysis

We conducted statistical analyses using R software (version 4.3.1). Univariate Cox regression analysis was used to determine prognostic genes. The Wilcoxon rank-sum test was utilized to compare the immune enrichment scores across differ-

ent groups. A *p*-value of < 0.05 was considered indicative of statistical significance.

Results

Establishment of immune escape-related gene model in osteosarcoma

Supplementary Figure S1 presents a schematic diagram of the overall analytical procedures for this study.

A univariate Cox regression analysis was conducted using the gene expression values of 182 immune escape (IE)-related genes as continuous variables in the TARGET cohort of patients with osteosarcoma having complete clinical survival data. This analysis calculated the hazard ratio for each gene. A *p*-value threshold of < 0.05 was set for selection, resulting in 47 genes meeting this criterion (Figure 1 A). Subsequent LASSO Cox regression analysis of these 47 genes determined the optimal number of genes based on lambda values corresponding to different gene counts. The analysis identified the most suitable number of genes as three: suppressor of cytokine signaling 1 (SOCS1), TNF receptor superfamily member 1A (TNFRSF1A), and autophagy related 7 (ATG7), demonstrating the minimum lambda values (Figures 1 B, C). The risk score model that predicts patient survival was then established by weighting the expression levels of these genes with their corresponding LASSO Cox regression coefficients: Risk score = (–0.2052093) × expression value of SOCS1 + (–0.1840314) × expression value of TNFRSF1A + (–0.1019449) × expression value of ATG7. We computed the risk score for each patient, revealing that the highest risk score was –3.526, the lowest was –5.968, and the median was –4.981. Utilizing this median risk score, we stratified the

A

	Hazard ratio (95% CI)	*P*-value
SOCS1	0.57 (0.43–0.77)	2.00E–04
TNFRSF1A	0.52 (0.37–0.74)	0.00028
ACTB	0.55 (0.39–0.79)	0.0012
FAS	0.69 (0.54–0.88)	0.0026
TMEM127	0.6 (0.43–0.85)	0.0042
ATG7	0.54 (0.35–0.83)	0.0048
PCED1B	0.7 (0.55–0.9)	0.0052
IFNGR	0.6 (0.41–0.87)	0.0065
PIGK	0.59 (0.4–0.87)	0.0074
HIRA	0.61 (0.42–0.88)	0.0082
PIGU	0.58 (0.38–0.87)	0.0084
TAP2	0.61 (0.42–0.89)	0.0094
IFNAR2	0.59 (0.39–0.89)	0.011
TGFBR2	0.7 (0.37–0.92)	0.011
TAPBP	0.61 (0.42–0.9)	0.012
HEXIM1	0.56 (0.36–0.88)	0.012
CHIC2	0.64 (0.45–0.91)	0.013
PIGS	0.65 (0.46–0.91)	0.013
TAP1	0.66 (0.48–0.93)	0.016
IFNGR2	0.59 (0.39–0.91)	0.016
MAPK1	0.63 (0.44–0.92)	0.016
PSMB9	0.75 (0.59–0.95)	0.017
NUP188	0.54 (0.33–0.9)	0.018
WDR7	0.62 (0.41–0.92)	0.018
DPH5	0.65 (0.45–0.93)	0.019
FNTB	0.57 (0.36–0.92)	0.02
TNFRSF1B	0.72 (0.54–0.95)	0.022
VPS35	0.61 (0.4–0.94)	0.024
STAT2	0.67 (0.487–0.95)	0.025
IST1	0.64 (0.43–0.95)	0.025
DNTTIP1	0.62 (0.4–0.95)	0.028
EMC8	0.67 (0.47–0.96)	0.028
PSMB8	0.76 (0.59–0.97)	0.031
DCP1A	0.58 (0.35–0.95)	0.031
PDCD6IP	0.61 (0.39–0.96)	0.031
RBCK1	0.69 (0.49–0.97)	0.033
FITM2	0.63 (0.41–0.97)	0.035
EMC3	0.64 (0.42–0.97)	0.037
B2M	0.75 (0.57–0.99)	0.039
ATXN7L3	0.57 (0.34–0.97)	0.039
NCBP1	0.65 (0.44–0.98)	0.039
PDSS2	0.62 (0.4–0.98)	0.04
ZC3H3	0.66 (0.44–0.99)	0.042
CREBBP	0.63 (0.41–0.99)	0.045
MED16	0.73 (0.53–1)	0.046
ATG12	0.59 (0.36–0.99)	0.047
USP7	0.65 (0.43–0.99)	0.047

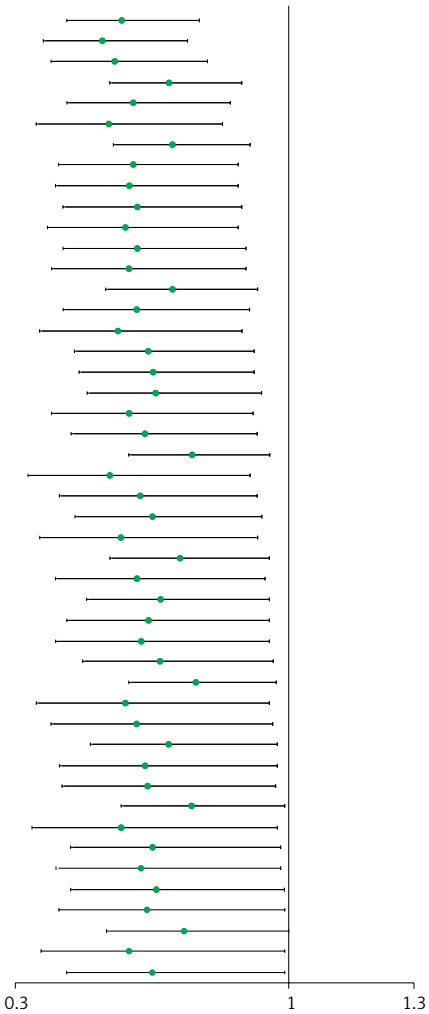

Figure 1. Prognostic prediction of patients with osteosarcoma using the immune escape-related gene model. **A** – Univariate Cox regression analysis results

LASSO – least absolute shrinkage, and selection operator, ROC – receiver operating characteristic, TARGET – Therapeutically Applicable Research to Generate Effective Treatments.

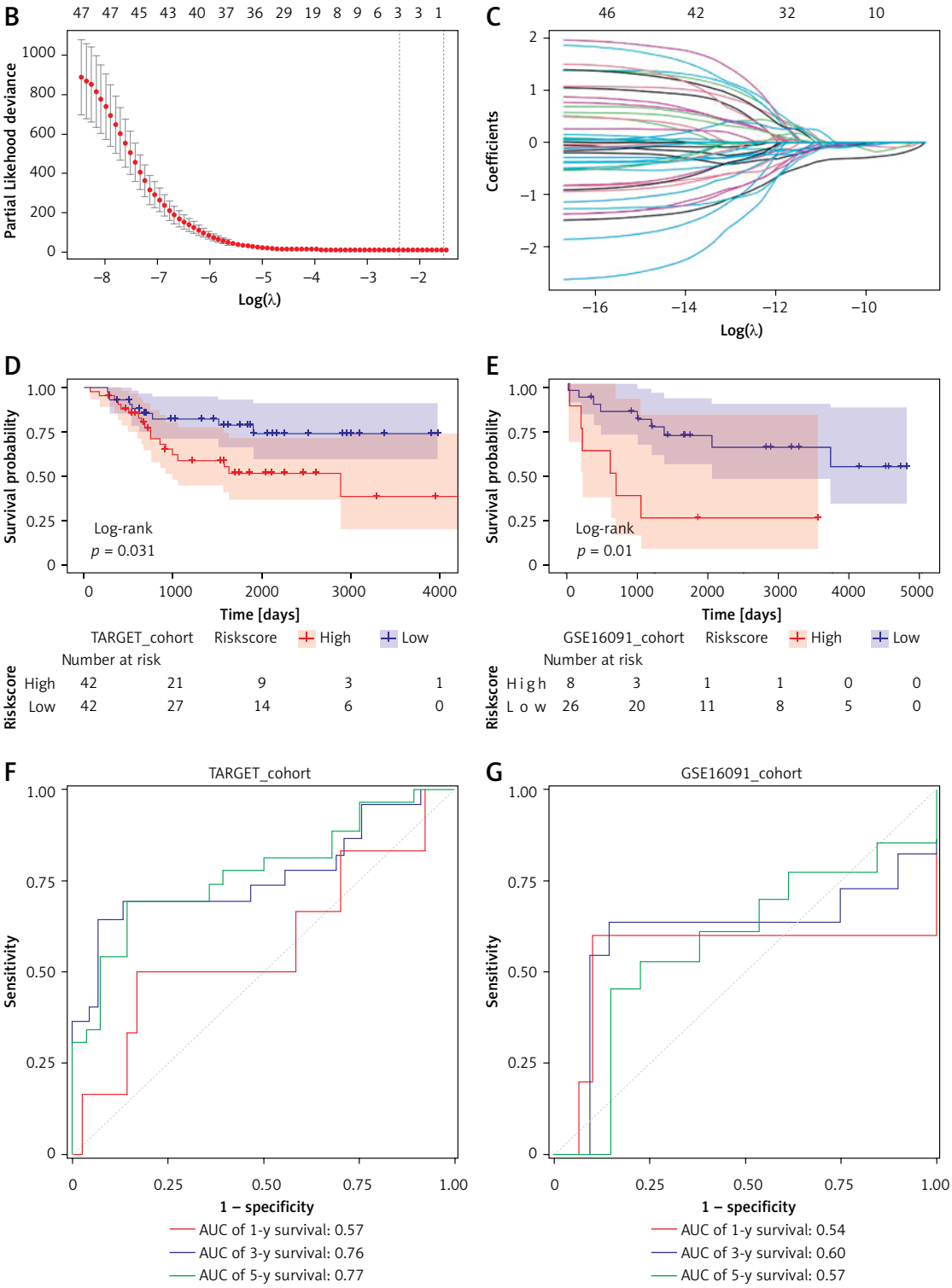

Figure 1. Cont. **B**, **C** – Lambda values from LASSO Cox regression analysis. **D** – Kaplan–Meier (K–M) survival curve for the TARGET dataset. **E** – K–M survival curve for GSE16091 dataset. **F** – ROC curve analysis for TARGET dataset. **G** – ROC curve analysis for the GSE16091 dataset

LASSO – least absolute shrinkage, and selection operator, ROC – receiver operating characteristic, TARGET – Therapeutically Applicable Research to Generate Effective Treatments.

osteosarcoma samples from the TARGET training set into high- and low-risk groups, with 42 samples in each group (Supplementary Table SII). Survival analysis emphasized a notably lower overall survival rate in the high-risk group compared to the low-risk group (Figure 1 D). The validity of this model was further reinforced by the GSE16091 dataset, which mirrored these results, indicating reduced overall survival in the high-risk group (Figure 1 E). Time-dependent ROC analysis underscored the model's predictive capability, with area under the curve values of 0.57, 0.76, and 0.77 in the training set (Figure 1 F) and 0.54, 0.60, and 0.57 in the validation set at 1, 3, and 5 years (Figure 1 G), affirming the model's effectiveness in forecasting the prognosis of patients with osteosarcoma based on TARGET data.

Prognostic value of the immune escape-related gene model in osteosarcoma

We analyzed its variation across different clinical characteristics (age, gender, and metastatic status) to investigate the clinical significance of the risk score. The analysis revealed no significant differences in risk scores between genders or between metastatic and nonmetastatic groups (Figures 2 A, B). However, the risk score was significantly higher in the < 18 age group compared to the ≥ 18 age group ($p < 0.05$) (Figure 2 C). Further, the prognostic relevance of the risk score in different clinical characteristics was evaluated. The results indicated that in the < 18 age group, osteosarcoma samples in the high-risk category exhibited poorer overall survival compared to those in the low-risk group ($p < 0.001$) (Figure 2 D). Similarly, high-risk osteosarcoma samples demonstrated worse overall survival than those in the low-risk group in the female group ($p < 0.001$) (Figure 2 E). Additionally, the high-risk category showed poorer overall survival outcomes compared to the low-risk group in the nonmetastatic group ($p < 0.001$) (Figure 2 F). This evidence indicates the use of the risk score as a differential prognostic indicator across various clinical demographics in osteosarcoma.

Predictive value of the immune escape-related gene model in the immune microenvironment of osteosarcoma

Our investigation focused on the association between the risk score and the prevalence of 28 distinct immune cell types within the TARGET cohort. The results revealed a substantial negative correlation of the risk score with central memory CD8 T cells, myeloid-derived suppressor cells, and macrophages. Conversely, a significant positive correlation was observed with gamma delta T cells, plasmacytoid dendritic cells, type 17 T helper cells, and eosinophils, among other immune cells, totaling 12 in number (Figures 3 A, B, Supplementary Table SIII). Furthermore, immune cell and functional analysis of high- and low-score groups revealed significant differences in aDCs, CCR, CD8 T cells, and Tregs among these groups (Figure 3 C). We calculated immune scores for the samples and categorized the osteosarcoma samples into high- and low-risk groups based on the median risk score using the TARGET cohort. The ESTIMATE Score, Immune Score, and Stromal Score were significantly higher in the low-risk group compared to the high-risk group (Figure 3 D). Additional correlation analyses between the risk score and the ESTIMATE Score, Immune Score, and Stromal Score revealed significant negative correlations (Figures 3 E–G). This emphasizes the robustness of the risk score as a predictive marker in the immune microenvironment of osteosarcoma, providing insights into the tumor's interaction with its immune milieu.

Differential pathways in samples with varying immune escape-related gene scores

The samples from the TARGET cohort were stratified into high- and low-risk groups based on the median risk score. We then conducted a differential gene expression analysis between these groups, focusing on genes with a *p*-value of < 0.05 and an absolute logFC of > 0.5. This identified 13,242 differentially expressed genes, comprising 82 that were upregulated and 13,160 that were downregulated (Figures 4 A, B). Significant insights emerged from the GO and KEGG enrichment analyses of these genes. The high-risk score group demonstrated notable enrichment in pathways such as Phototransduction, Various types of N-glycan biosynthesis, N-glycan biosynthesis, and Arachidonic acid metabolism, in the KEGG analysis. Conversely, 165 pathways, including those related to Salmonella infection, Autophagy – animal, and Alzheimer's disease, were significantly enriched in the low-risk score group (Figure 4 C). Similarly, the GO enrichment analysis revealed that pathways such as fibroblast growth factor receptor signaling, midbrain development, and cellular response to fibroblast growth factor stimulus were significantly enriched in the high-risk score group. In contrast, the low-risk score group demonstrated predominant enrichment in 3,194 pathways, including proteasome-mediated ubiquitin-dependent protein catabolic process, macroautophagy, and protein localization to organelle establishment (Figure 4 D). Additionally, GSVA results indicated significant enrichment in 74 pathways, including GOBP_INTERLEUKIN_2_MEDIATED_SIGNALING_PATHWAY and GOCC_DEATH_INDUCING_SIGNALING_COM-

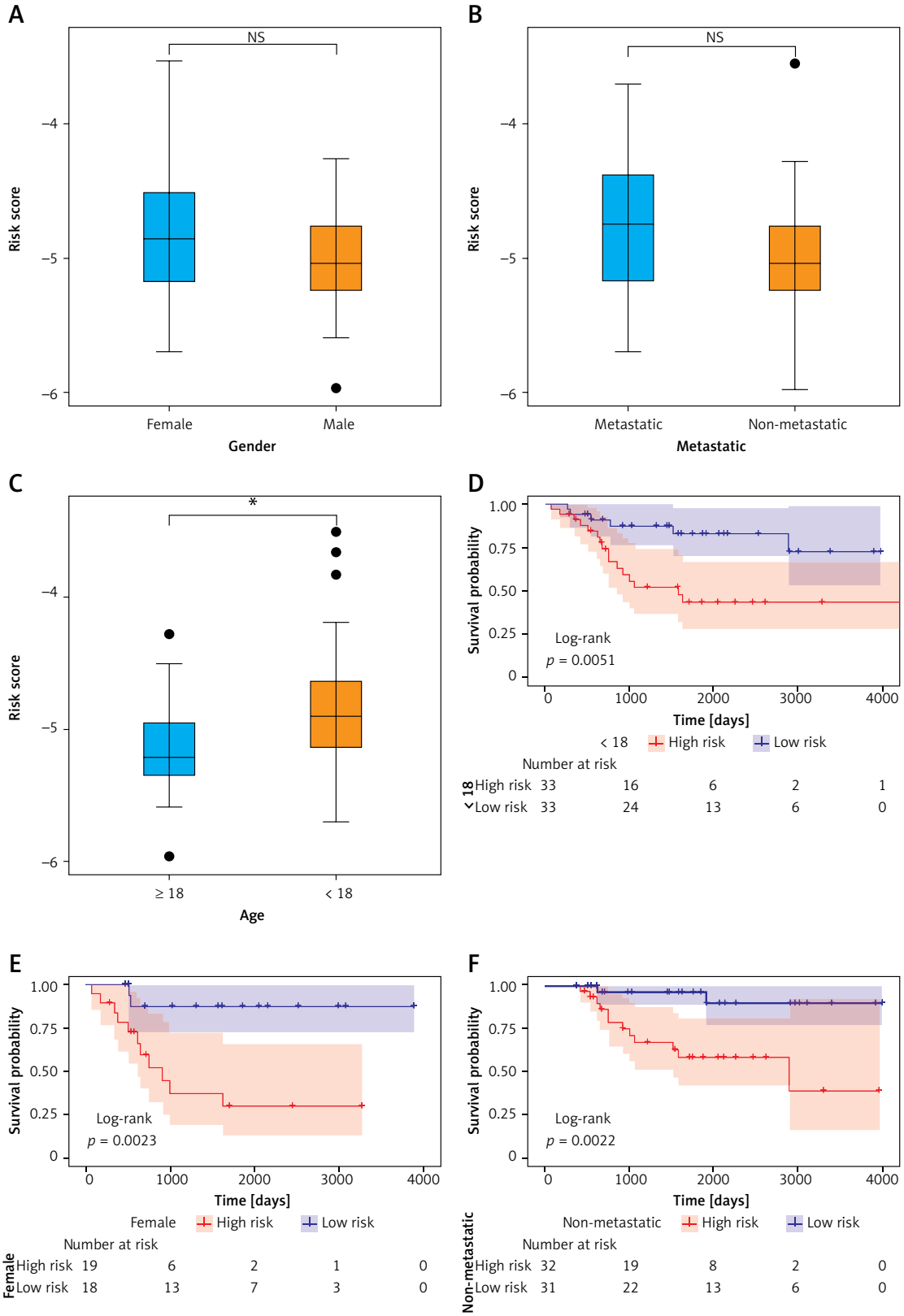

Figure 2. Prognostic potential of the immune escape-related gene model in osteosarcoma. **A** – Variation of risk score by gender. **B** – Variation of the risk score in metastatic versus nonmetastatic groups. **C** – Variation of risk score across different age groups. **D** – K–M survival curve for the < 18 age group. **E** – K–M survival curve for the female gender group. **F** – K–M survival curve for the nonmetastatic group

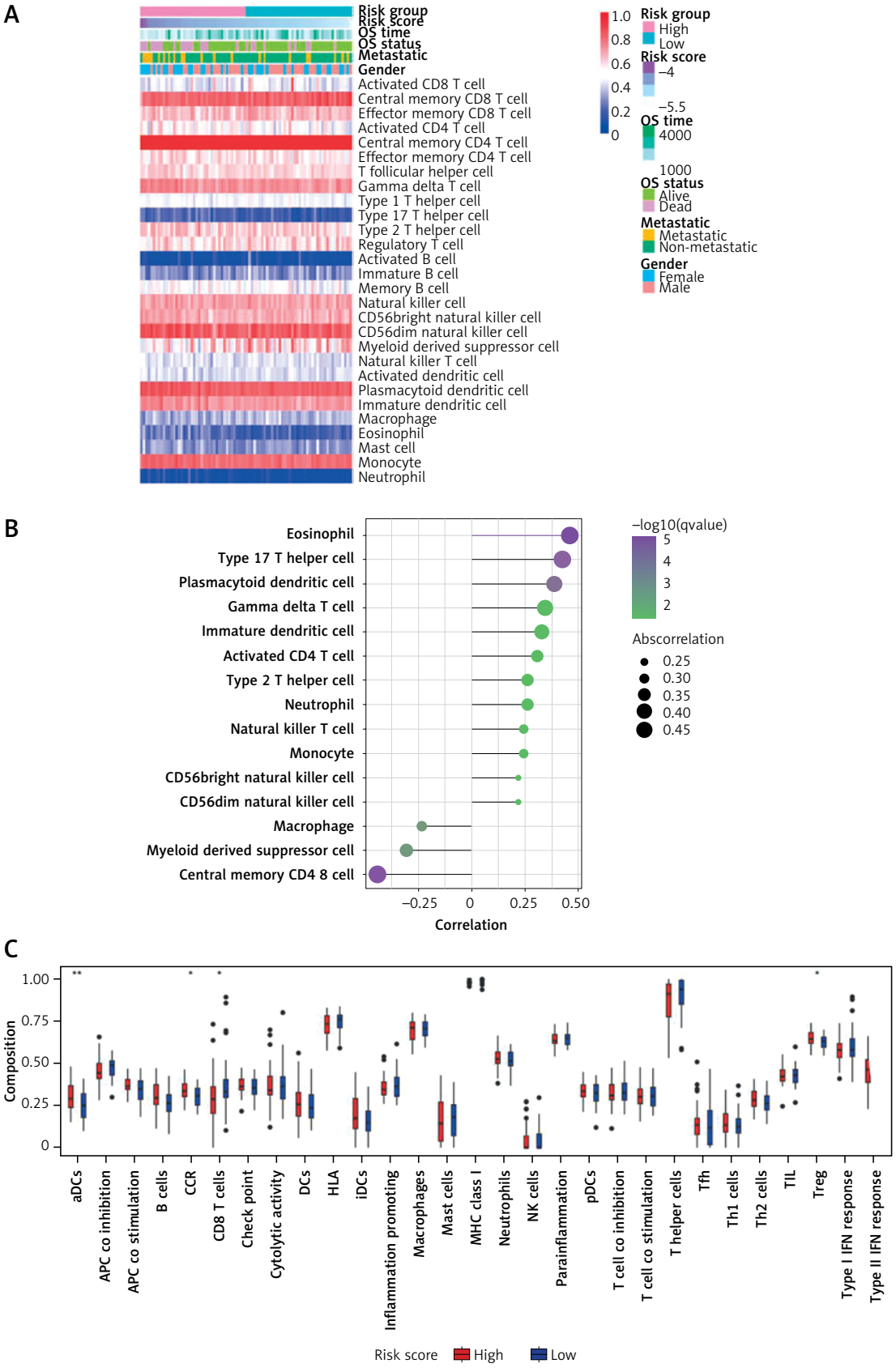

Figure 3. Predictive potential of the immune escape-related gene model in the tumor immune microenvironment of osteosarcoma. **A** – Heatmap demonstrating immune infiltration of 28 specific immune cell types. **B** – Correlation plot depicting the association between risk score and the 28 immune cell types. **C** – Differences in 29 types of immune cells and functions between the high- and low-risk score groups

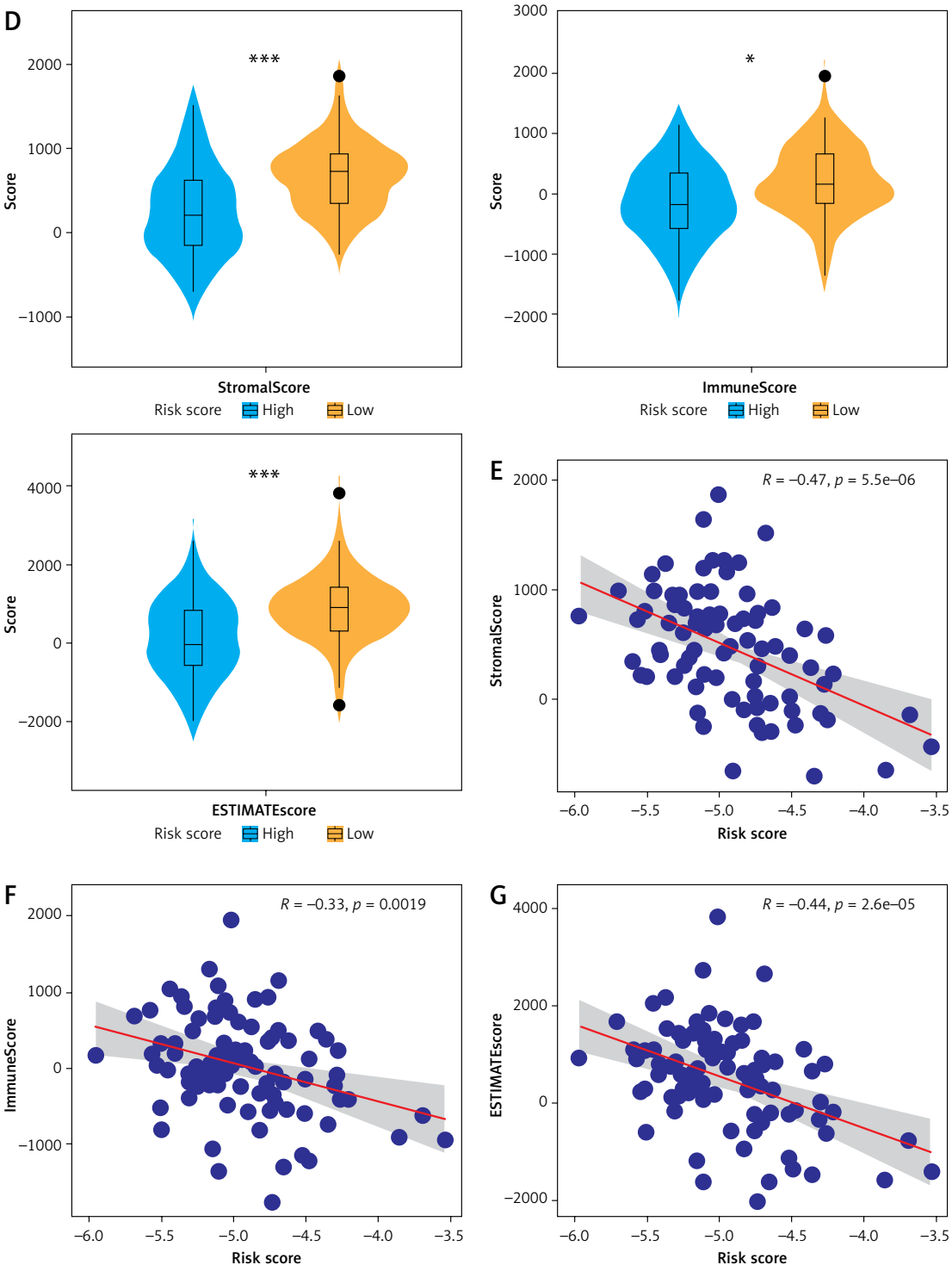

Figure 3. Cont. **D** – Violin plots indicating differences in StromalScore, ImmuneScore, and ESTIMATEScore between the high- and low-risk score groups. Scatter plots denoting the correlation of risk score with StromalScore (**E**), ImmuneScore (**F**), and ESTIMATEScore (**G**)

PLEX (Figure 4 E). Supplementary Table SIV presents detailed results of all enrichment analyses. This comprehensive pathway analysis emphasizes the complex molecular interactions and biological processes associated with varying immune escape levels in osteosarcoma.

Predictive value of immune escape-related gene scores in osteosarcoma treatment response

Drug sensitivity prediction in the TARGET cohort was performed with the "oncoPredict"

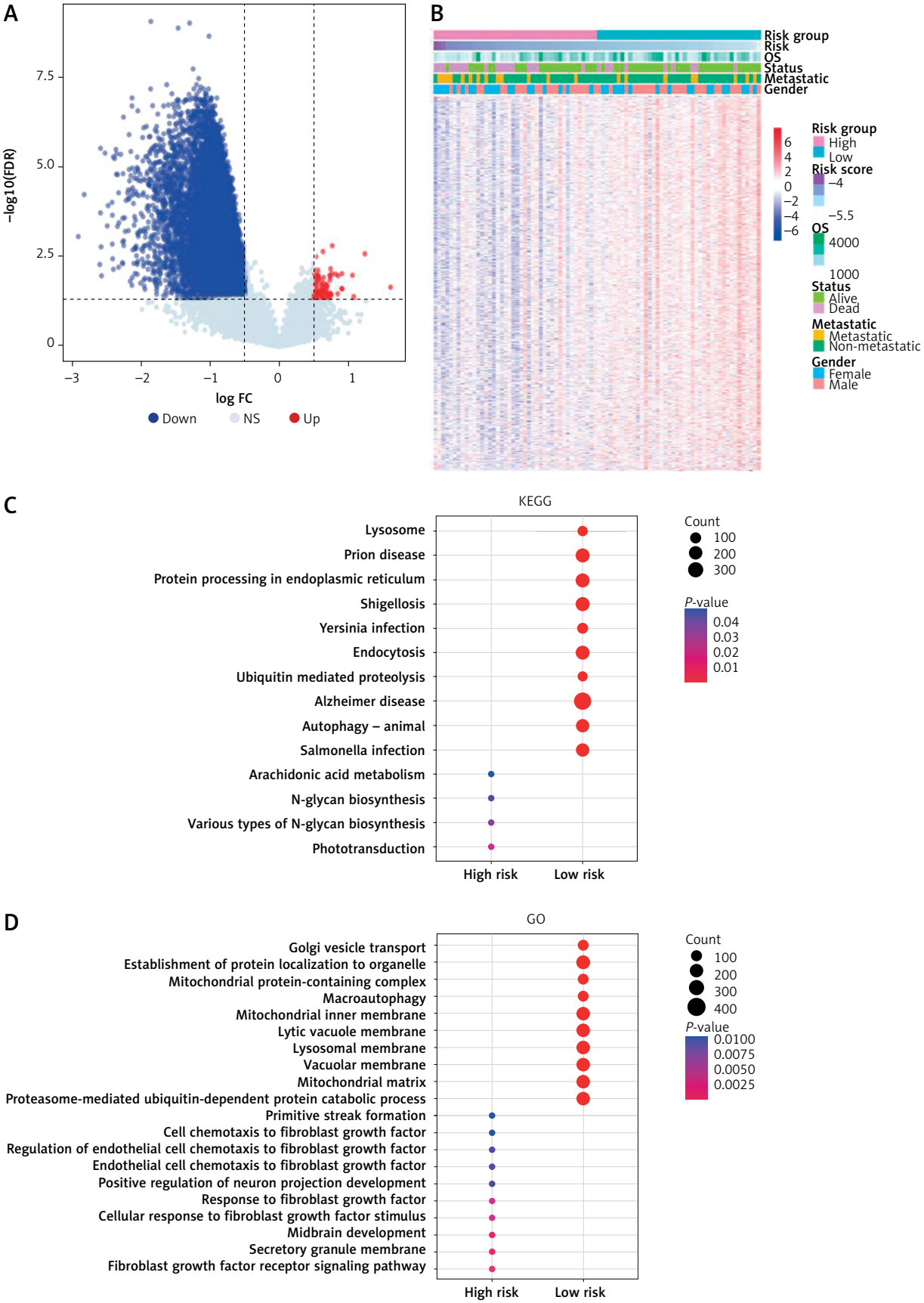

Figure 4. Pathway enrichment analysis in the high- and low-risk score groups. **A** – Volcano plot illustrating differentially expressed genes. **B** – Heatmap of differentially expressed genes. Results of KEGG (**C**) and GO (**D**) enrichment analyses comparing the high- and low-risk score groups

KEGG – Kyoto Encyclopedia of Genes and Genomes, GO – Gene Ontology, GSVA – gene set variation analysis, OS – overall survival.

Figure 4. Cont. **E** – GSVA results comparing the high- and low-risk score groups, risk score, OS time, OS status, metastatic status, and gender

KEGG – Kyoto Encyclopedia of Genes and Genomes, GO – Gene Ontology, GSVA – gene set variation analysis, OS – overall survival.

package in R [18]. We analyzed the correlation between the risk score and the IC_{50} of various drugs. The results revealed that the risk score had a significant positive correlation with 175 drugs, including XAV939_1268, AZ960_1250, and AZD1332_1463 (Figure 5 A). Conversely, a significant negative correlation was found with 3 drugs, including SB505124_1194, BI.2536_1086, and ABT737_1910 ($p < 0.05$, Figure 5 B, Supplementary Table SV). This result indicates that the immune escape-related gene score is a potential biomarker for predicting the efficacy of specific therapeutic agents in osteosarcoma, thereby helping in treatment strategy customization.

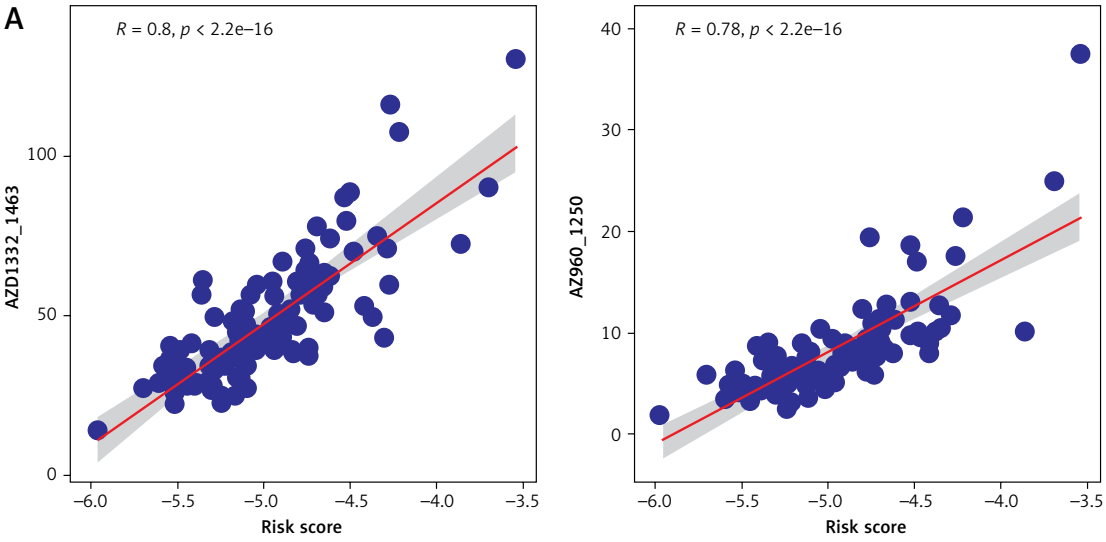

Figure 5. Predictive potential of the immune escape-related gene model in the drug correlation of osteosarcoma. Scatter plots showing positive (**A**) correlations between risk score and various drugs

PCA – principal component analysis, KEGG – Kyoto Encyclopedia of Genes and Genomes, GO – Gene Ontology.

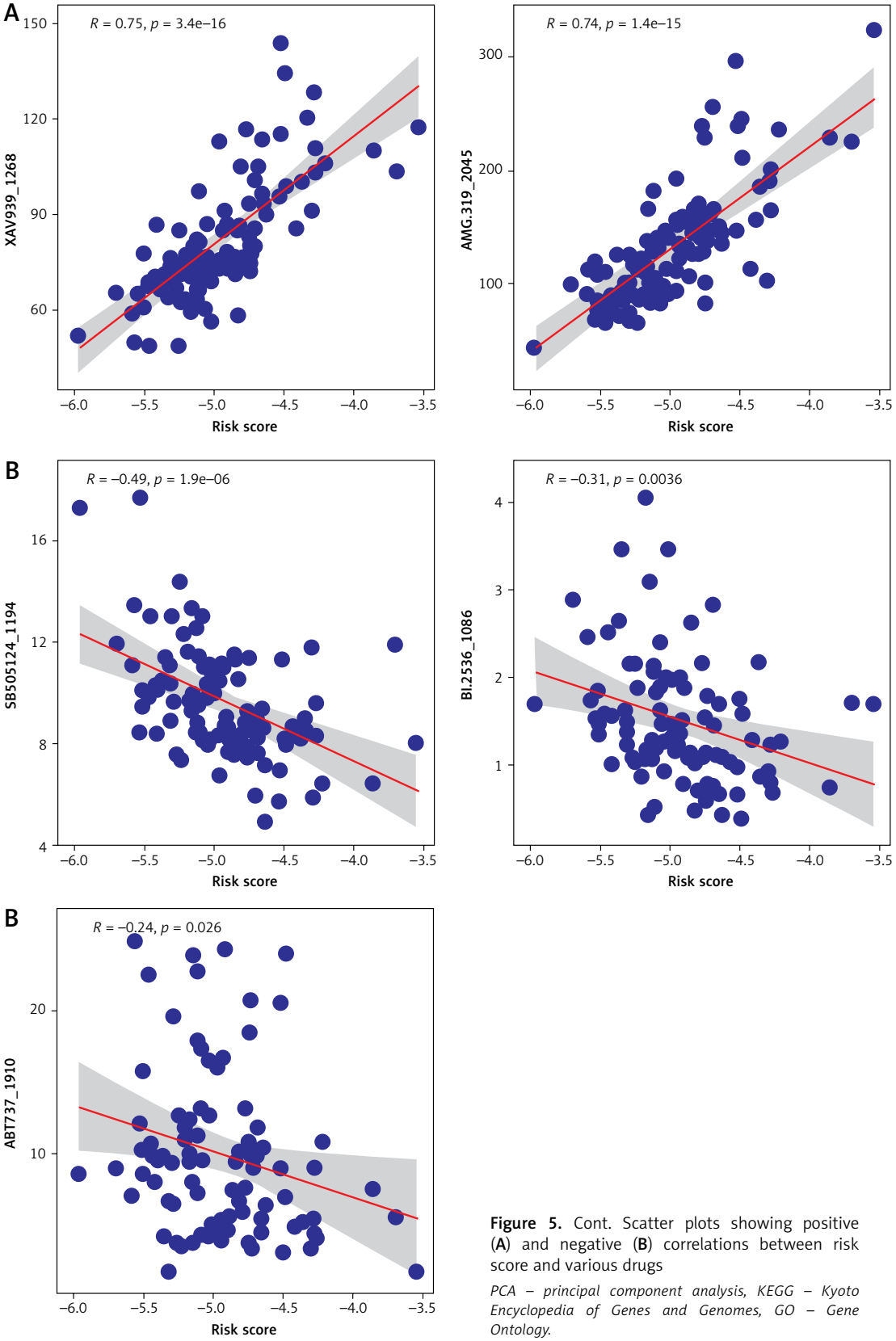

Figure 5. Cont. Scatter plots showing positive (**A**) and negative (**B**) correlations between risk score and various drugs

PCA – principal component analysis, KEGG – Kyoto Encyclopedia of Genes and Genomes, GO – Gene Ontology.

Analysis of immune escape-related gene scores in single-cell data of osteosarcoma

We obtained single-cell gene expression profiles using three samples from the GSE162454 single-cell sequencing dataset. These profiles were used for subsequent analyses after data processing and filtration. PCA was conducted (Figure 6 A) with 5,000 variable genes to reduce dimensionality, and 19 cell clusters were determined with Seurat (Supplementary Figure S2). Figure 6 B shows cell annotation results. The levels of immune escape-related gene scores in identified cells were determined (Figure 6 C), and Supplementary Figure S3 shows sample distribution results.

Differential expression genes between high- and low-scoring groups of immune escape-related gene scores were determined based on the FindMarkers results, using the criteria of an avg_log2FC absolute value of > 0.5 and a *p*-value of < 0.05. Enrichment analysis for these differentially expressed genes was conducted with GO and KEGG pathways. KEGG enrichment results indicated significant enrichment in pathways such as rheumatoid arthritis, interleukin-17 signaling pathway, lysosome, osteoclast differentiation, bladder cancer, arginine, and proline me-

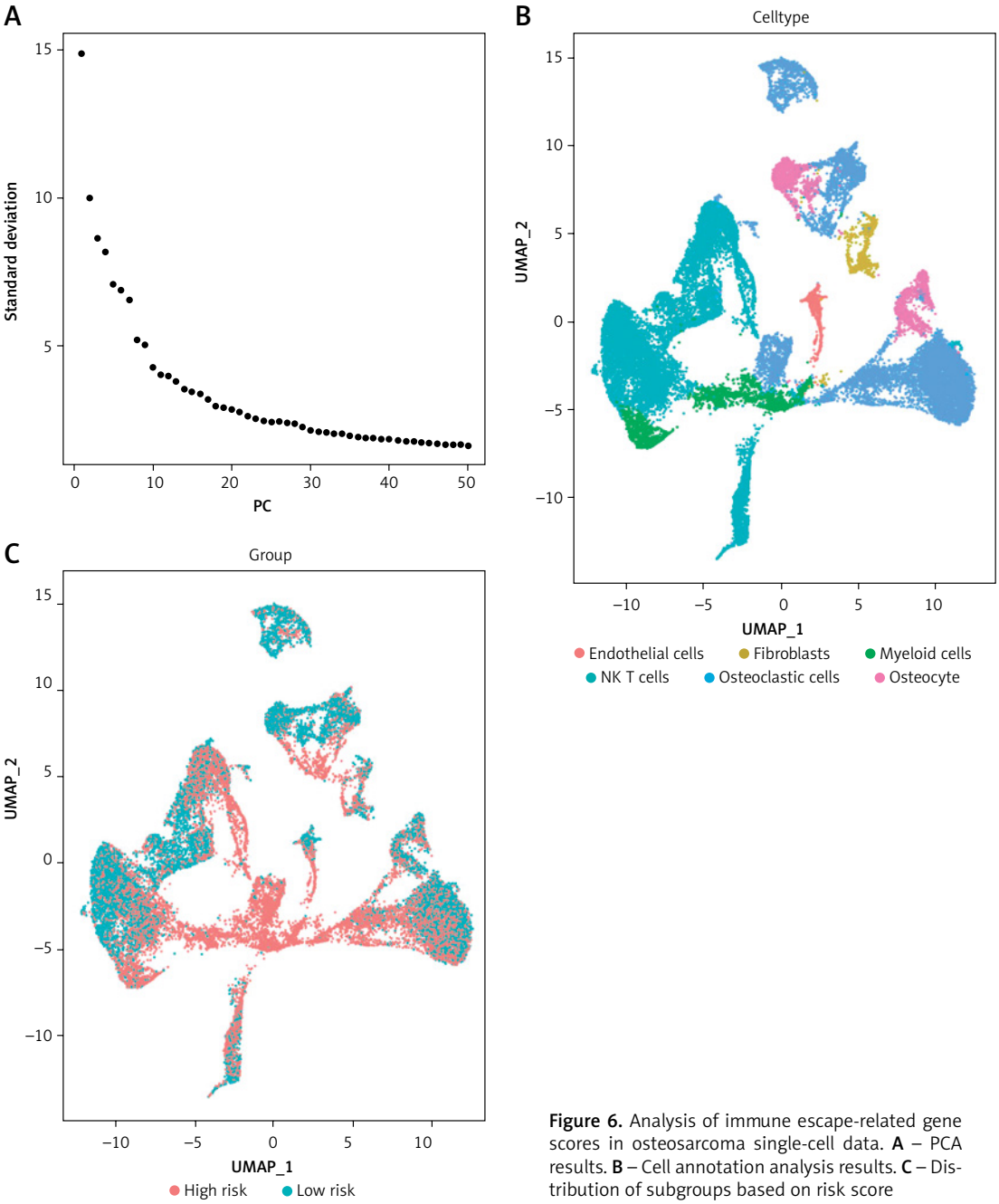

Figure 6. Analysis of immune escape-related gene scores in osteosarcoma single-cell data. **A** – PCA results. **B** – Cell annotation analysis results. **C** – Distribution of subgroups based on risk score

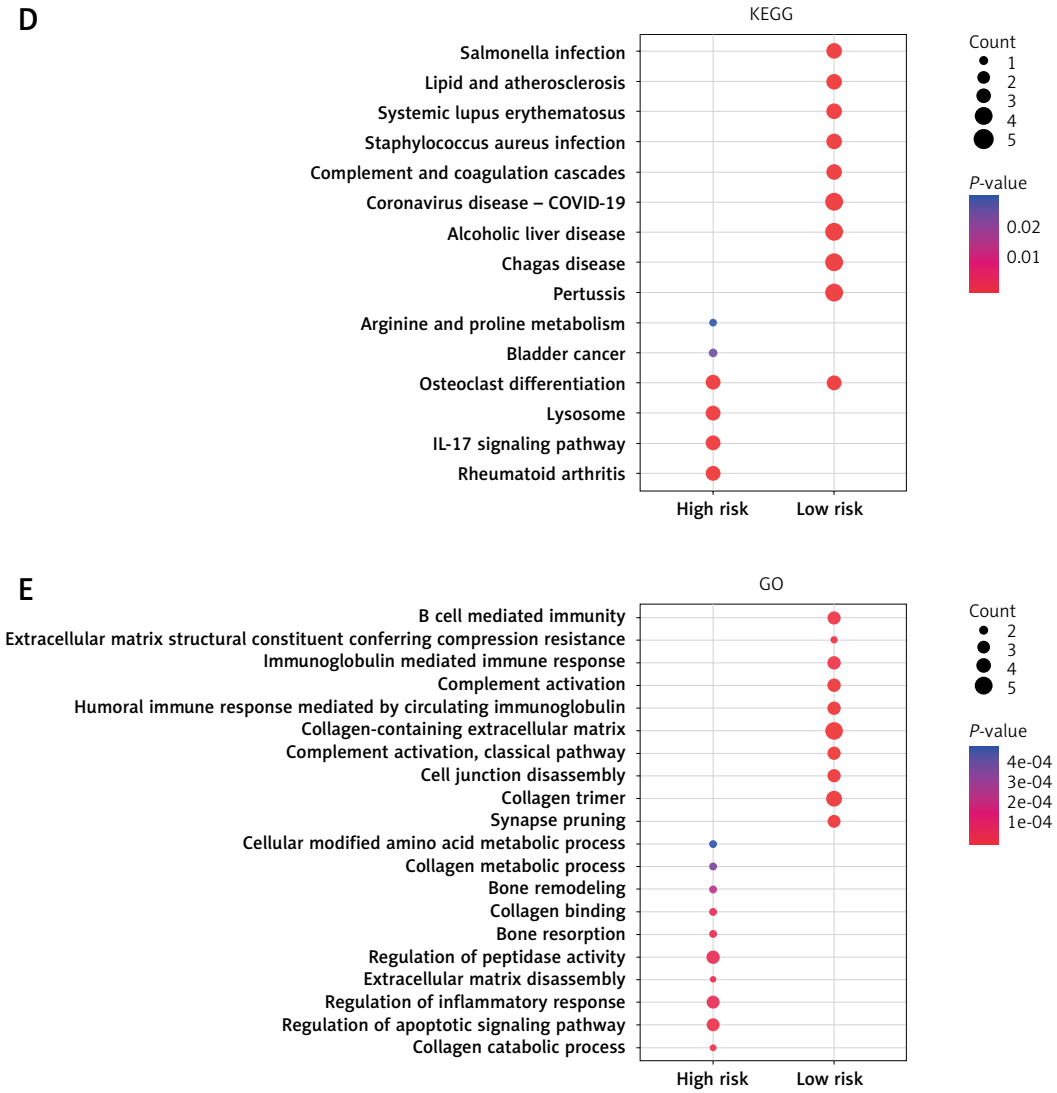

Figure 6. Cont. **D** – KEGG enrichment analysis results for the high- and low-risk score groups in single-cell data. **E** – GO enrichment analysis results for the high- and low-risk score groups in single-cell data

tabolism in the high-scoring group. In contrast, pathways such as pertussis, Chagas disease, alcoholic liver disease, and 29 others, were significantly enriched in the low-scoring group (Figure 6 D). GO enrichment results revealed significant enrichment in 224 pathways, including collagen catabolic process, apoptotic signaling pathway regulation, inflammatory response regulation in the high-scoring group, and 250 pathways, such as synapse pruning, collagen trimer, and cell junction disassembly, in the low-scoring group (Figure 6 E). Supplementary Table SVI shows detailed results of these enrichment analyses. This comprehensive analysis emphasizes the intricate molecular mechanisms at play in the immune escape landscape of osteosarcoma at the single-cell level.

Cell communication landscape associated with immune escape-related gene scores in osteosarcoma

We analyzed intercellular communication among subgroups of immune escape-related genes using iTALK, focusing on checkpoints, cytokines, and growth factors. Among growth factors, immune escape-related genes, such as platelet derived growth factor C (PDGFC), transforming growth factor β1 (TGFB1), and syndecan 2 (SDC2), were the most abundant, indicating active signaling pathways in osteosarcoma (Figure 7 A, B). The immune escape-related gene interleukin 1 receptor (IL1R) was highly expressed in osteosarcoma in the realm of cytokines, representing another active signaling pathway (Figures 7 C, D). Within checkpoints, CD24 molecule (CD24) and TNF superfamily

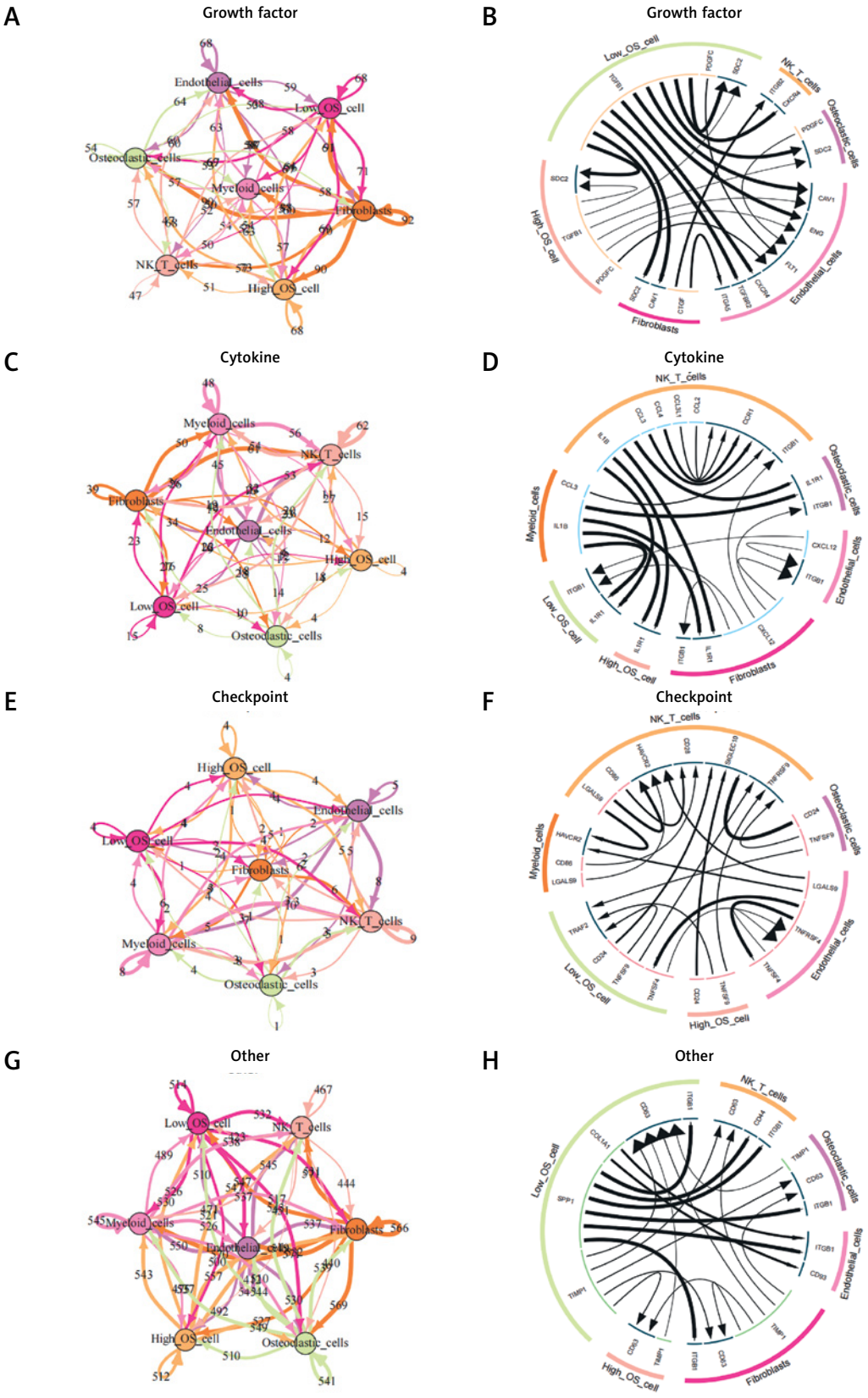

Figure 7. Cell communication analysis based on immune escape-related gene scores in osteosarcoma. **A**, **B** – Cell communications between growth factors and subgroups of immune escape-related gene scores. **C**, **D** – Cell communications between cytokines and subgroups of immune escape-related gene scores. **E**, **F** – Cell communications between checkpoints and subgroups of immune escape-related gene scores. **G**, **H** – Cell communications between other and subgroups of immune escape-related gene scores

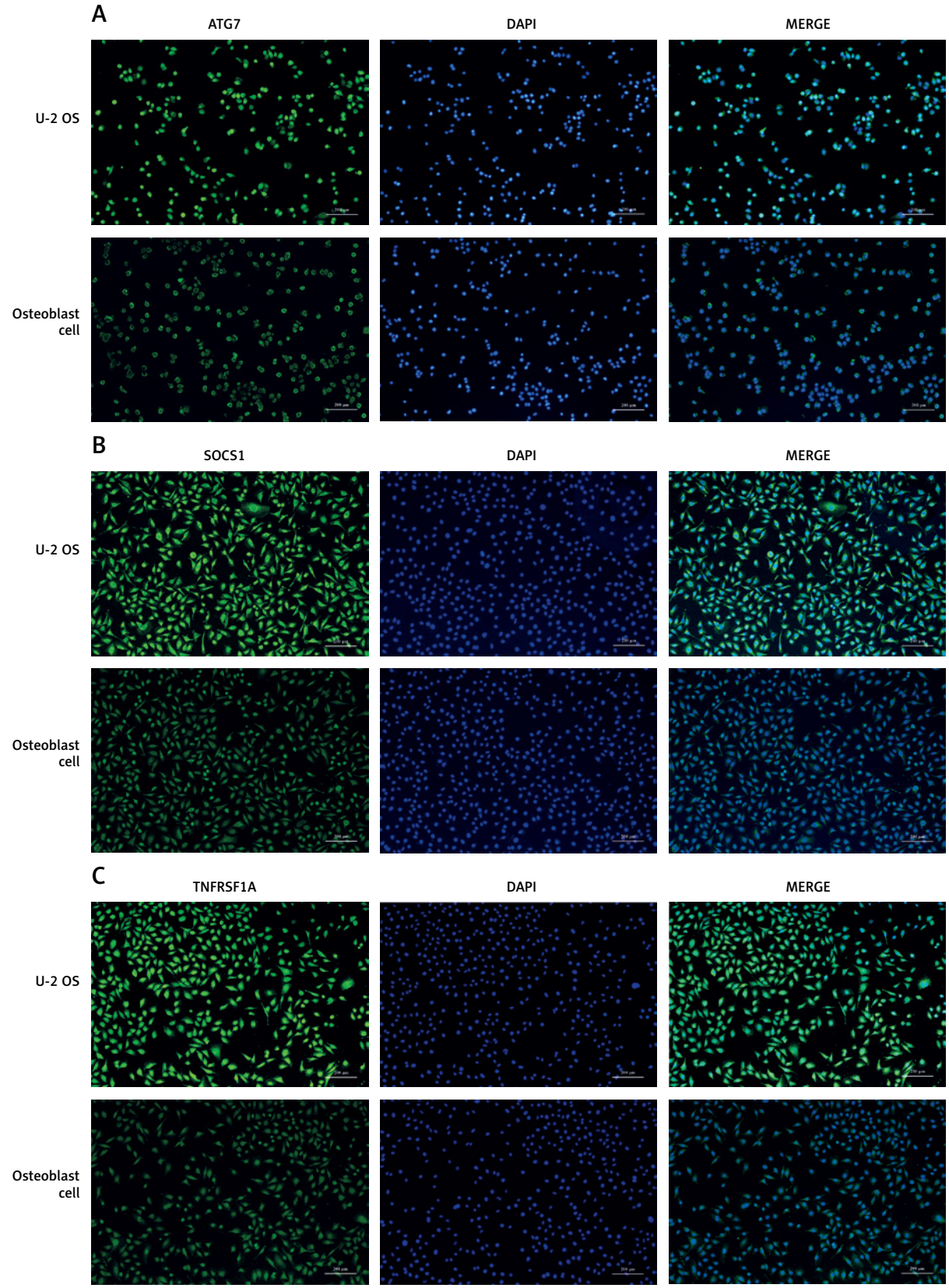

Figure 8. Immunofluorescence images depicting the expression of proteins encoded by immune escape-related genes in osteosarcoma cells. **A** – Immunofluorescence images of ATG7 protein. **B** – Immunofluorescence images of SOCS1 protein. **C** – Immunofluorescence images of TNFRSF1A protein. Scale bar: 200 µm

member 9 (TNFSF9), associated with high immune escape-related gene scores, were determined as active signaling pathways in osteosarcoma (Figures 7 E, F). CD63 molecule (CD63) and TIMP metallopeptidase inhibitor (TIMP) in the "other" module were highly expressed and interacted with other immune escape-related genes such as TGFB1 and SDC2 (Figures 7 G, H). Overall, these results indicate the intricate interplay between immune escape-related genes through growth factors and checkpoint signaling pathways in osteosarcoma, verifying the complex communication networks within the tumor microenvironment.

Expression of proteins encoded by immune escape-related genes in osteosarcoma

To experimentally validate the expression levels of immune escape-related genes in osteosarcoma cells, we further conducted an immunofluorescence staining analysis. As illustrated in Figures 8 A–C, the protein expression levels of ATG7, SOCS1, and TNFRSF1A were all significantly upregulated in the osteosarcoma cell line U-2 OS compared to those in osteoblast cells. The findings from the experimental validation conducted via immunofluorescence assays substantiate the accuracy of the osteosarcoma risk score model developed through the machine learning technique.

Discussion

Osteosarcoma, as a prevalent malignant bone tumor, is known for its complex immune microenvironment and mechanisms of immune escape, which have long been focal points in cancer research [19]. This study introduces an immune escape-related gene model developed to predict the prognosis of patients with osteosarcoma and investigate the characteristics of their immune microenvironment [20]. Our research focuses on identifying genes that are significantly associated with the survival prognosis of patients with osteosarcoma and constructing a risk-scoring model based on these genes. We have successfully developed an immune escape-related gene model for predicting the prognosis of patients with osteosarcoma and analyzed its role in the immune microenvironment. This is congruent with the study of Alexander *et al*., who determined the key role of SOCS1 in regulating immune responses [21]. Additionally, the roles of TNFRSF1A and ATG7 in tumor immune escape are supported by another study [9], emphasizing the importance of determining key immune escape genes in osteosarcoma. Studies have revealed that TNFRSF1A plays a role in tumor cell survival and immune surveillance evasion through its interaction with tumor necrosis factor-α (TNF-α). TNF-α is a proinflammatory cytokine that activates the nuclear factor kappa-light-chain-enhancer of the activated B-cell signaling pathway in tumor cells, thereby promoting tumor growth and immune escape [6, 8].

Our research, based on a risk score model derived from these genes, reveals that patients in the high-risk group demonstrated a poorer survival prognosis. This result is congruent with other studies that have revealed the significance of immune gene signatures in predicting the survival of patients with cancer [22]. Further analysis of the immune microenvironment revealed a correlation between the risk score and specific immune cell types. Additionally, several studies have determined the role of immune cells within the tumor microenvironment [23]. These results emphasize the importance of immune cells in osteosarcoma progression. Differential pathway analysis revealed significant molecular distinctions between the high-risk and low-risk groups. Similarly, other studies have determined comparable molecular pathway differences in osteosarcoma [24]. These discoveries regarding differential pathways provide new perspectives in understanding the molecular mechanisms of osteosarcoma. Moreover, our study investigates the potential value of immune escape-related gene scoring in predicting treatment responses, indicating potential biomarkers for personalized treatment strategies. Our study provides a comprehensive understanding of the immune evasion mechanisms of osteosarcoma at the single-cell level. We determined patterns of immune evasion through single-cell analysis, demonstrating that immune cells play a pivotal role in either suppressing or promoting tumor growth. This involvement may include specific types of T cells, macrophages, or other immune cells [25]. Moreover, our results expose alterations in intracellular signaling pathways within tumor cells that may facilitate their survival and proliferation while evading the immune system's assault. Recent research supported these discoveries. In particular, one study, using single-cell transcriptomics, revealed the complexity of the untreated osteosarcoma tumor microenvironment, further emphasizing the diversity and intricacy of immune cells within the tumor milieu [26]. Another study focused on the immunosuppressive function of regulatory T cells in osteosarcoma, demonstrating their significant role in tumor immune evasion [27]. Additionally, research using single-cell RNA sequencing techniques has disclosed the identity and heterogeneity of malignant osteoblasts and the tumor microenvironment in osteosarcoma, helping in the understanding of how tumor cells survive and proliferate under immune attack [9]. These research results not only resonate with our

conclusions but also enrich the understanding of the immune evasion mechanisms in osteosarcoma, particularly in the single-cell analysis context.

Our study has limitations despite providing valuable information. First, our results warrant validation in a broader population due to sample size and data source constraints. Second, our study predominantly relies on retrospective data, and prospective studies are required to further validate these results.

Overall, our research provides new information for prognostic prediction and immune microenvironment analysis in osteosarcoma by developing a risk-scoring model based on immune escape-related genes. Our results not only reveal the crucial role of immune escape genes in osteosarcoma progression but also indicate potential biomarkers for future personalized treatment strategies. Additionally, the single-cell analysis deepens our understanding of osteosarcoma's immune escape mechanisms. Our study provides essential insights, but further research is warranted to validate these results and explore their clinical application potential.

In conclusion, the present study developed a risk scoring model for osteosarcoma based on immune escape-related genes. Its capacities of prognostic prediction, immune microenvironment assessment, and drug treatment response prediction were examined, thereby confirming its robust predictive performance. Moreover, the model was further validated through the utilization of single-cell sequencing data. The model we established can effectively predict the prognosis, immune status, and drug response of osteosarcoma patients by thoroughly investigating the immune escape mechanisms. Consequently, it provides a valuable tool for predicting the overall characteristics of osteosarcoma and establishes a theoretical framework for personalized precision treatment of this malignant tumor.

Funding

Yunnan Orthopedic Trauma Clinical Medical Center(No. ZX20191001); Yunnan Orthopedics and Sports Rehabilitation Clinical Medicine Research Center (No. 202102AA310068); Research on Injury Treatment and Accelerated Rehabilitation in Joint Operations in Tropical Mountains and Jungles(War Office [2022]250).

Ethical approval

Not applicable.

Conflict of interest.

The authors declare no conflict of interest.

References

1. Niu J, Yan T, Guo W, et al. Identification of potential therapeutic targets and immune cell infiltration characteristics in osteosarcoma using bioinformatics strategy. Front Oncol 2020; 10: 1628.
2. Redondo A, Cruz J, Lopez-Pousa A, Barón FJC, SEOM. SEOM clinical guidelines for the treatment of osteosarcoma in adults-2013. Clin Transl Oncol 2013; 15: 1037-43.
3. Xie QK, Zhao YJ, Pan T, et al. Programmed death ligand 1 as an indicator of pre-existing adaptive immune responses in human hepatocellular carcinoma. Oncoimmunology 2016; 5: e1181252.
4. Wildes TJ, Dyson KA, Francis C, et al. Immune escape after adoptive T-cell therapy for malignant gliomas. Clin Cancer Res 2020; 26: 5689-700.
5. Chen Y, Xu J, Wu X, et al. CD147 regulates antitumor CD8+ T-cell responses to facilitate tumor-immune escape. Cell Mol Immunol 2021; 18: 1995-2009.
6. Lu C, Klement JD, Smith AD, et al. p50 suppresses cytotoxic T lymphocyte effector function to regulate tumor immune escape and response to immunotherapy. J Immunother Cancer 2020; 8: e001365.
7. Yu L, Zhang J, Li YJ. Effects of microenvironment in osteosarcoma on chemoresistance and the promise of immunotherapy as an osteosarcoma therapeutic modality. Front Immunol 2022; 13: 871076.
8. De Jaeghere EA, Denys HG, De Wever O. Fibroblasts fuel immune escape in the tumor microenvironment. Trends Cancer 2019; 5: 704-23.
9. Zhou Y, Yang D, Yang QC, et al. Single-cell RNA-seq reveals identity and heterogeneity of malignant osteoblast cells and TME in osteosarcoma. bioRxiv 2020; 2020.04. 16.044370.
10. Fan TM, Roberts RD, Lizardo MM. Understanding and modeling metastasis biology to improve therapeutic strategies for combating osteosarcoma progression. Front Oncol 2020; 10: 13.
11. Grünewald TG, Alonso M, Avnet S, et al. Sarcoma treatment in the era of molecular medicine. EMBO Mol Med 2020; 12: e11131.
12. Gill J, Gorlick R. Advancing therapy for osteosarcoma. Nat Rev Clin Oncol 2021; 18: 609-24.
13. Lu Y, Zhang J, Chen Y, et al. Novel immunotherapies for osteosarcoma. Front Oncol 2022; 12: 830546.
14. Ritchie ME, Phipson B, Wu D, et al. limma powers differential expression analyses for RNA-sequencing and microarray studies. Nucleic Acids Res 2015; 43: e47.
15. Yoshihara K, Shahmoradgoli M, Martínez E, et al. Inferring tumour purity and stromal and immune cell admixture from expression data. Nat Commun 2013; 4: 2612.
16. Hao Y, Hao S, Andersen-Nissen E, et al. Integrated analysis of multimodal single-cell data. Cell 2021; 184: 3573-87.e29.
17. Wang Y, Wang R, Zhang S, et al. iTALK: an R package to characterize and illustrate intercellular communication. bioRxiv 2019:507871.
18. Maeser D, Gruener RF, Huang RS. oncoPredict: an R package for predicting in vivo or cancer patient drug response and biomarkers from cell line screening data. Brief Bioinform 2021; 22: bbab260.
19. Zhu XG, Chudnovskiy A, Baudrier L, et al. Functional genomics in vivo reveal metabolic dependencies of pancreatic cancer cells. Cell Metab 2021; 33: 211-21.e6.
20. Chavez-Dominguez R, Perez-Medina M, Lopez-Gonzalez JS, Galicia-Velasco M, Aguilar-Cazares D. The double-edge sword of autophagy in cancer: from tumor

suppression to pro-tumor activity. Front Oncol 2020; 10: 578418.
21. Lu J, Tang H, Chen L, et al. Association of survivin positive circulating tumor cell levels with immune escape and prognosis of osteosarcoma. J Cancer Res Clin Oncol 2023; 149: 13741-51.
22. Guo J, Tang H, Huang P, et al. Single-cell profiling of tumor microenvironment heterogeneity in osteosarcoma identifies a highly invasive subcluster for predicting prognosis. Front Oncol 2022; 12: 732862.
23. Lei X, Lei Y, Li JK, et al. Immune cells within the tumor microenvironment: biological functions and roles in cancer immunotherapy. Cancer Lett 2020; 470: 126-33.
24. Liu W, Hu H, Shao Z, et al. Characterizing the tumor microenvironment at the single-cell level reveals a novel immune evasion mechanism in osteosarcoma. Bone Res 2023; 11: 4.
25. Liu Y, Feng W, Dai Y, et al. Single-cell transcriptomics reveals the complexity of the tumor microenvironment of treatment-naive osteosarcoma. Front Oncol 2021; 11: 709210.
26. Griffin KH, Thorpe SW, Sebastian A, et al. Engineered bone marrow as a clinically relevant ex vivo model for primary bone cancer research and drug screening. Proc Natl Acad Sci USA 2023; 120: e2302101120.
27. Cheng D, Zhang Z, Mi Z, et al. Deciphering the heterogeneity and immunosuppressive function of regulatory T cells in osteosarcoma using single-cell RNA transcriptome. Comput Biol Med 2023; 165: 107417.